

Dissolution of polymer films in supercritical carbon dioxide using a quartz crystal microbalance

Yazan Hussain, You-Ting Wu, Paa-Joe Ampaw, Christine S. Grant*

Department of Chemical and Biomolecular Engineering, NC State University, Raleigh, NC 27695-7905, United States

Received 17 June 2006; received in revised form 20 March 2007; accepted 24 March 2007

Abstract

The dissolution kinetics of polymeric materials in CO₂ is crucial to the understanding, design and control of CO₂-based environmentally benign lithography processes. This study utilizes the quartz crystal microbalance (QCM) to monitor and evaluate the dissolution of poly(1,1-dihydroperfluorooctyl methacrylate-*r*-2-tetrahydropyranyl methacrylate), poly(FOMA-*r*-THPMA), polymer films in supercritical CO₂ over a range of temperatures and pressures. Polymer dissolution rates at the range of pressures studied were evaluated to quantify the dissolution kinetics for the polymer. The experiments revealed that the polymer dissolution in supercritical CO₂ undergoes two apparent processes: a rapid absorption of CO₂ into the polymer film followed by a gradual dissolution of polymer film into the CO₂ at the polymer–CO₂ interface. The nature of these interfacial phenomena and their associated effect on the rate are discussed.

© 2007 Elsevier B.V. All rights reserved.

Keywords: Quartz crystal microbalance; Polymer dissolution; Carbon dioxide; Sorption; Fluoropolymer

1. Introduction

Polymer dissolution is an important phenomenon in many industrial processes including membranes synthesis, plastics recycling, drug delivery applications, and photolithography [1]. For example, in this last application the dissolution of CO₂ soluble polymer based films is critical to controlling the ultimate features in the final device. However, the organic solvents used in these processes have a negative impact on the environment and have produced pressure on industry to reduce utilization of these hazardous materials [2]. In addition, for applications where the polymer is to be used in therapeutic applications, *e.g.*, drug delivery, it is important to eliminate the residual solvents from the final product [3]. As a result, attention in the last decade had been given to supercritical fluids, especially CO₂, as a potential replacement for traditional organic solvent processes. However, there are still some challenges associated with the commercialization of this new technology. In the case of photolithography the challenge has been to develop industrially relevant CO₂-soluble photoactive polymers and a CO₂-based lithography process that are compatible with existing device requirements.

When compared to other solvents such as halogenated organics, CO₂ is non-toxic, non-flammable and is considered a green chemical [4]. Industrial attention to supercritical CO₂ is due to its availability, modest critical conditions ($T_c = 31\text{ }^\circ\text{C}$, $P_c = 1071\text{ psi}$), tunable dissolving power and high diffusivity, in addition to being environmentally benign [5,6]. However, the poor solvency of CO₂ to most polymers had limited the implementation of this emerging technology [7]. As a result, considerable effort has been made, since the early 1990's, toward improving polymer solubility in CO₂ leading to the modification of fluoropolymers and polyethers to produce highly CO₂-soluble polymers [8–10].

The behavior of polymers in solvents depends on both energetic and entropic effects, which, in turn, depend on the chemical structure and polymer conformation [11]. While the CO₂ power as a solvent is complex and cannot be easily predicted from mere consideration of chemical structure, the availability of dissolution studies on polymers with different structures in CO₂ can provide a considerable insight into its solvency phenomenon [12]. Previous studies have provided many examples that demonstrate how different chemical and physical properties, such as side chain length, backbone stiffness, and polarity, affect a polymer's behavior in CO₂ [13–15].

On the other hand, while the development of different supercritical carbon dioxide (scCO₂) processes has been an active

* Corresponding author. Tel.: +1 919 515 2317; fax: +1 919 515 3465.
E-mail address: grant@ncsu.edu (C.S. Grant).

Nomenclature

C_m	QCM constant (frequency–mass conversion)
Δm	mass change
m_{dis}	calculated change in mass during the dissolution stage at P_{exp}
m_f	net mass of polymer removed
m_0	initial mass of polymer on crystal
P_c	critical pressure
P_{exp}	pressure at which polymer dissolution starts
P_m	intermediate pressure, before dissolution stage
S	CO ₂ solubility in polymer
t_{exp}	time taken during the polymer dissolution stage
T_c	critical temperature

Frequency notation

F_0	frequency of blank crystal
ΔF_{CO_2}	change in frequency due to CO ₂ adsorption
ΔF_f	change in frequency corresponding to m_f
ΔF_m	change in frequency due to mass change
ΔF_p	change in frequency due to pressure change
ΔF_T	change in frequency due to temperature change
ΔF_η	change in frequency due to viscosity change
F^x	frequency at pressure x

Greek letters

μ_q	quartz shear modulus = $2.947 \times 10^{11} \text{ g cm}^{-1} \text{ s}^{-2}$
ρ_q	quartz density = 2.648 g cm^{-3}

area of research, analytical techniques aimed at the *in situ* characterization of organic films have been limited [16]. Techniques that have been used for the conventional processes suffer from being complicated to use or require long equilibration times [17]. These techniques include the high pressure ellipsometry [18], interferometric dissolution rate monitors [16], and other gravimetric techniques [19].

The objective of this work is to study the behavior of a fluorinated copolymer in CO₂ under different temperatures and pressures. This work focuses on the mechanisms associated with adsorption, swelling, and dissolution of CO₂-soluble polymer thin films (in the sub-micron region).

2. Nanoscale microweighing at high pressures

Most conventional microbalances such as spring, beam and torsional balances, have a sensitivity of about 10^{-6} g, and in most cases, are not designed for application in extreme pressure conditions [19]. In contrast, the quartz crystal microbalance (QCM) has a sensitivity reaching 10^{-9} g and can serve as a powerful tool for *in situ* microweighing in high pressure environments [19,20].

A search of the current literature indicates that there are a limited number of studies using the QCM in high pressure systems. The first study to apply the QCM microweighing under high pressure was by Bonner and Cheng who studied the sorption

of N₂ in polyethylene (PE) at 125 °C and show a good agreement between their results and those from literature obtained by the pressure decay technique [17]. Otake et al. determined the mass of CO₂, N₂ and He adsorbed onto a silver QCM surface at 40 °C and pressures up to 5800 psi [21]. Aubert reported the solubility of CO₂ in a variety of polymers such as polystyrene (PS), poly(methyl methacrylate) (PMMA), and Teflon at 35 and 40 °C and pressures up to 1500 psi using the QCM technique [20]. Miura et al. studied the solubility and adsorption of CO₂ in PS at 40 °C and pressures up to 2500 psi [22]. In their work, the expected amount of CO₂ adsorbed on the surface was estimated by measuring the total solubility of CO₂ at different pressures for three PS films with different initial mass. Guigard et al. evaluated the adsorption of CO₂ on the gold electrode surface of a QCM and extended the use of QCM to determine the solubility of *bis*(acetylacetonato) copper(II) and *bis*(thenoyltrifluoroacetonnato) copper(II) in CO₂ at 40 °C and 1500 psi [23]. Zhang et al. studied the sorption of CO₂ into glassy PMMA films at different temperatures [24]. Other QCM studies include an evaluation of the inclusion behavior of guest molecules to a solid apohost in scCO₂ [25], and probing the vapor–liquid critical point of pure and mixed fluids [26,27].

The authors have also used the QCM system developed in this study to examine different polymer systems at high pressures. In a previous publication, the QCM system utilized in this study was used to examine the sorption of CO₂ into glassy and rubbery PMMA films to evaluate a theoretical model developed to predict sorption of small molecules in polymers [28]. The kinetics of the CO₂/PMMA sorption process was investigated as well in a separate work. We have also used the QCM to examine the anomalous sorption of CO₂ into thin PMMA films and the supercritical impregnation of drugs into polymers [29].

Up to this point microweighing studies that have been performed on polymers under high pressure conditions, especially CO₂, have only observed sorption phenomenon. No studies were found on the dissolution kinetics of polymer films in high pressure CO₂. However, utilizing the QCM in polymer dissolution studies in liquid is more common, *e.g.*, the study reported by Hinsberg et al. [30] who investigated the dissolution of three different polymers in tetramethylammonium hydroxide. References to other studies that utilized a QCM to investigate polymer dissolution can be found in the paper by Ito [31]. This manuscript demonstrates the utilization of the QCM for similar dissolution studies under supercritical conditions.

The measured variable of the QCM is the frequency. The change in this frequency is a function of several system variables including changes in mass, pressure, and surrounding solution properties. In general, the total frequency change can be written as:

$$\Delta F = F - F_0 = \Delta F_m + \Delta F_p + \Delta F_\eta \quad (1)$$

where the terms on the right hand side represent the change in frequency due to mass loading, ΔF_m ; pressure, ΔF_p and viscosity, ΔF_η . The following relations are usually used for the

different terms [32–34]:

$$\Delta F_m = \frac{-2F_0^2}{(\mu_q \rho_q)^{1/2}} \Delta m = -C_m \Delta m \quad (2)$$

$$\Delta F_p = C_p P \quad (3)$$

$$\Delta F_\eta = -0.5 C_m (\pi F_0)^{1/2} (\rho_f \eta_f)^{1/2} \quad (4)$$

where C_m is the mass sensitivity constant ($56.6 \text{ Hz } \mu\text{g}^{-1} \text{ cm}^{-2}$ for a 5 MHz crystal), Δm is the mass per unit area, μ_q and ρ_q are the shear modulus and density of the quartz, C_p is a constant equal to 0.34 Hz/psi, and ρ_f and η_f are the density and shear viscosity of the fluid medium surrounding the crystal. Viscous loading on the crystal also causes an increase in energy dissipation through viscous coupling, which can be detected by measuring the crystal resistance. The relationship between resistance and solution properties is given as [35]:

$$\Delta R = \frac{\pi n}{8K^2 C_0} \left(\frac{\rho \eta}{\pi F_0 \mu_q \rho_q} \right)^{1/2} \quad (5)$$

where n is the number of crystal faces exposed to the fluid, K^2 the quartz electromechanical coupling coefficient and C_0 is the static capacitance of the crystal. Viscous coupling can occur with the surrounding fluid as well as the polymer overlayer due to its viscoelastic nature. While Eq. (4) can predict the effect of the fluid on the frequency, quantifying the contribution from film viscoelasticity to ΔF is difficult. Fortunately, this non-gravimetric effect can be neglected with reasonable accuracy for films thinner than $0.2 \mu\text{m}$ [36].

Other factors that can affect the QCM frequency include temperature and surface roughness. Since all the experiments reported in this study were isothermal, the temperature effect will not be considered. Details on this effect can be found in the literature [37,38]. Surface roughness can affect the frequency in two ways. First, the entrapment of the fluid within the surface crevices can cause an increase in the mass load but will have small effect on energy dissipation. The second factor is the non-shear coupling generated by the movement of the surface asperities in the fluid, which will contribute to the energy dissipation [39]. This study assumes that the effect of surface roughness is negligible based on the fact that, for surfaces with few nanometer RMS roughness, this contribution is only a few Hertz and is not expected to change significantly during the course of the experiment [40]. This assumption is also consistent with the aforementioned thin film studies, and is acceptable when relatively large frequency changes are being considered compared to that expected due to surface roughness.

3. Experimental

3.1. Materials

Poly(1,1-dihydroperfluorooctyl methacrylate-*r*-2-tetrahydropyranyl methacrylate), poly(FOMA-*r*-THPMA), a random copolymer with 65 mol% FOMA and 35 mol% THPMA (Fig. 1), was used in this study. The polymer was synthesized

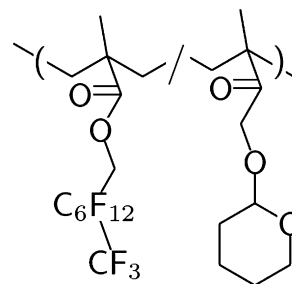


Fig. 1. Poly(FOMA-*r*-THPMA).

and purified by the DeSimone research group at UNC-Chapel Hill [41]. This polymer has a molecular weight of 15 kDa and a T_g of 48°C in its pure form (no CO_2). Trifluorotoluene (TFT) of greater than 99% purity was purchased from Aldrich Chemical Company and used as received. Coleman grade (purity > 99.99%) CO_2 was obtained from National Welders.

3.2. QCM system

The quartz crystals used in this study were 5.00 MHz AT-cut. The crystals, as obtained by International Crystal Manufacturing (ICM), had a blank diameter of 8.5 mm and a thickness of 0.25 mm. A Si film (3.5 mm diameter and $0.1 \mu\text{m}$ thickness) was vacuum sputtered over an Au electrode; the gold provides the necessary electrical actuation to the quartz. The RMS surface roughness for the crystals is less than 10 nm (analyzed using Atomic Force Microscopy [40]). The crystal is connected to an oscillator circuit (Maxtek model PLO-10). This oscillator provides two outputs, frequency and voltage; the voltage reading is inversely proportional to the crystal's resistance. The frequency from the oscillator is read by an Agilent 225 MHz Universal Frequency Counter (model 53131A). Temperature, pressure, voltage, and frequency readings are acquired using LabView.

3.3. Pressure cell and apparatus

The custom-built pressure cell was a thick-walled cylinder (ID 63.5 mm \times 200 mm), with a high-pressure electrical feedthrough (Conax Buffalo Technologies) at the top end to drive the QCM. The cell had an inside volume of 25 cm^3 and a maximum working pressure of 7500 psi. During an experiment the crystal was placed into the cell and connected to the oscillator through the electrical feedthrough. A high-pressure thermocouple (Omega Engineering Inc.) was placed in the cell to monitor the temperature. The pressure inside the cell was monitored using a pressure transducer (Omega Engineering Inc.) with an accuracy of 0.02% of the reading. The whole assembly was then placed in a water bath and controlled to $\pm 0.1^\circ\text{C}$. The required pressure was achieved via an ISCO pump (model 260D, ISCO, Inc.) which can provide pressures up to 7500 psi. A complete description of the system can be found elsewhere [28].

3.4. Methods

3.4.1. Polymer film preparation

An 8.0 wt.% polymer solution was prepared by dissolving 0.8 g of solid polymer into 9.2 g of TFT solvent. Prior to coating the polymer film on the crystal, a clean crystal was placed into the pressure cell to determine the fundamental frequency, F_0 , in vacuum at the experiment temperature. The vacuum condition (less than 0.004 psi) was realized using a precision model DD-20 vacuum pump (VWR Scientific Products). A polymer film was then cast onto the surface of the crystal by dipping the crystal into the PFOMA/TFT solution for a short time (about 1 min) then withdrawing it at a controlled speed via a variable speed motor which (the speed) controls the initial polymer mass on the crystal. The coated crystal was then placed back into the pressure cell and dried at the run temperature under vacuum until no frequency change was observed. The value of the stabilized frequency of the coated QCM in vacuum was utilized to calculate the initial total mass of coated polymer.

3.4.2. Cell pressurization

In contrast to its utilization under atmospheric conditions, the use of QCM under high pressures is more challenging due, primarily, to the high mechanical disturbances associated with the large changes in pressure. The selection of experimental conditions for polymer dissolution under high pressures requires the controlled addition of CO_2 into the pressure cell. The initial approach for determining the polymer dissolution at constant temperature and pressure was to instantaneously add CO_2 to the cell. However, such fast addition of CO_2 can cause a very high shear force acting on the crystal which causes the frequency to be strongly biased by this sudden mechanical stress. This highly irregular signal may last up to 2 min causing the loss of the most critical part of a dissolution curve; the initial response. As a result, the instantaneous addition of CO_2 to the required dissolution pressure was unrealistic experimentally. An alternative to this fast pressurization was to gradually add CO_2 to avoid the aforementioned difficulty while establishing a high pressure baseline. However, this may cause the film dissolution to start before the required pressure for the experiment is reached.

Experiments showed that a combination of gradual and instantaneous addition of CO_2 significantly reduces the shear force acting on the crystal while maintaining a constant pressure during dissolution experiments. This was achieved by a gradual injection of CO_2 to an intermediate pressure (P_m) lower than the dissolution pressure (P_{dis}), followed by a rapid addition of CO_2 to the experimental pressure (P_{exp}) as shown in Fig. 2. This second step (from P_m to P_{exp}) usually takes 20–30 s.

After careful consideration of the dissolution behavior within this pressure range, a value of 1110 psi was selected for P_m ; this selection has several advantages. First, the selected P_m is close to the pressure at which dissolution begins (P_{dis}) minimizing the effect of large, fast pressure changes. Second, since CO_2 is already in the supercritical state for the range

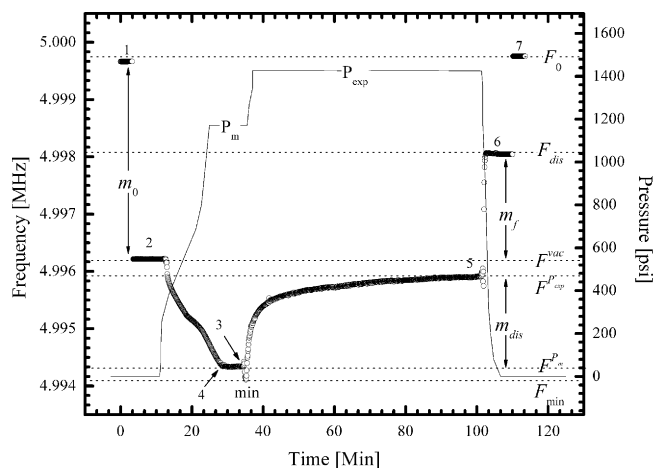


Fig. 2. Frequency of QCM coated with PFOMA film ($\sim 0.3 \mu\text{m}$) in CO_2 at 37°C (circles) as a function of time during the pressure cycle (solid line).

of temperature considered in this study, it avoids any phase transition upon further injection of CO_2 into the cell instantly to achieve the value of P_{exp} . Finally, it enables one to establish equilibrium between CO_2 sorption and desorption in the polymer film before dissolution occurs. As a result, this equilibrium will minimize the net contribution of CO_2 mass to frequency.

3.5. Film dissolution evaluation

In the studies reported here, the dissolution of the polymer film in CO_2 occurred over a 10–60 min time period depending upon the operating conditions. Following dissolution, the CO_2 was rapidly bled out of the cell while the frequency of the crystal was continuously recorded. Once atmospheric pressure is reached, the QCM was disconnected and the remaining polymer was removed by washing in a pure TFT solvent. Finally, the dried crystal was put back into the cell to determine the frequency for comparison with the uncoated crystal frequency (F_0). The fundamental frequency of the crystal could be usually recovered to within 3.0 Hz of the original uncoated value; this indicates the ability to close the material balance on the film.

4. Results and discussion

A typical run is presented in Fig. 2 to show the different stages (*i.e.*, coating, swelling, dissolution) of the experiment. In the following discussion, F_0 will refer to the frequency of the uncoated crystal under vacuum. The steady state frequency of the crystal with the polymer film at a certain pressure (*e.g.*, vacuum, 1425 psi, or P_m) will be designated as F^x , where the superscript x indicates the pressure (*e.g.*, F^{vac} , F^{1425} , or F^{P_m}) associated with the surrounding fluid. A full list of the nomenclature is also provided. The initial mass of the polymer film can be calculated from the initial frequency change, *i.e.*, $F_0 - F^{vac}$, using the Sauerbrey Eq. (2) as $m_f = (F_0 - F^{vac})/C_m$.

During the course of the dissolution process several phenomena take place as shown schematically by Fig. 3. Initially, CO_2 will be adsorbed on the polymer film surface; a process that

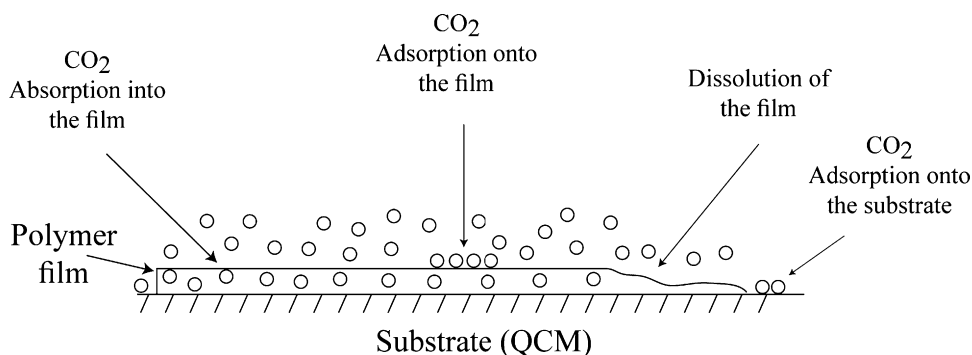


Fig. 3. Schematic showing the different phenomena involved during the dissolution process of polymer films.

occurs on a short time scale such that its effect on the QCM response will be competing with the pressure effect. Therefore, the frequency increase due to the pressure increase, as suggested by Eq. (3), will be depressed due to the mass adsorbed on the surface. Following adsorption, CO₂ will start to diffuse inside the polymer film causing the frequency to decrease due to the mass increase. This diffusion process happens on a much longer time scales and can be easily followed by the QCM as discussed below. The sorption process will also induce stresses inside the polymer which will eventually start to relax resulting in a change in the polymer film viscoelastic properties which might affect the QCM response as discussed in the following section. As the CO₂ concentration inside the polymer increases, a critical concentration is reached where the polymer chains will have enough mobility to entangle from the network which marks the onset of the dissolution starts.

4.1. Film viscoelasticity

The frequency difference between F^{vac} and F^{P_m} (recall that P_m is the intermediate pressure where dissolution has not started yet) represents all possible contributions to the frequency that includes pressure, CO₂ viscosity and density, polymer film viscoelasticity, and CO₂ uptake. At this initial stage the polymer film is swollen by the absorbed CO₂ which would result in a change in polymer film viscoelasticity. To test the extent to which the QCM response is affected by changes in the viscoelasticity, the change in resistance (ΔR) for uncoated and coated crystals was measured. The results shown in Fig. 4 are for ΔR over a range of pressures (including the supercritical transition) and at temperatures below and slightly above the T_g . As can be seen from Fig. 4(a) the change in the resistance did not show significant difference between the coated and uncoated crystals; the temperature is the main parameter in ΔR shift. In Fig. 4(b), the data in Fig. 4(a) is represented as a function of the CO₂ density–viscosity product to show that the linear relation between ΔR and $(\rho\eta)^{0.5}$, as suggested by Eq. (5), is indeed obtained. It is therefore concluded that the viscous coupling is predominately caused by CO₂ and not by the polymer film. Thus, Eq. (4) is expected to take into account the non-gravimetric contribution to frequency change due to this viscous coupling. Again, this can be attributed to the small thickness of the polymer film ($\sim 0.3 \mu\text{m}$) as discussed earlier.

4.2. Sorption-dominated stage

If the frequency change due to polymer film is designated as ΔF_f ; the frequency change due to CO₂ absorption will be $S\Delta F_f$, where S is the solubility in gram CO₂/gram polymer. Then, Eq.

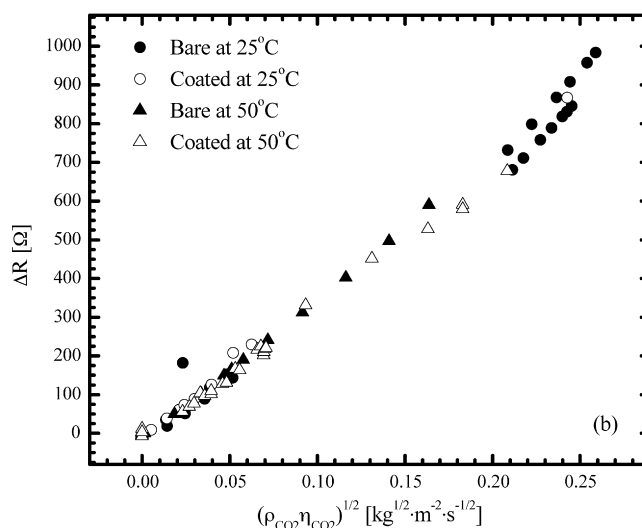
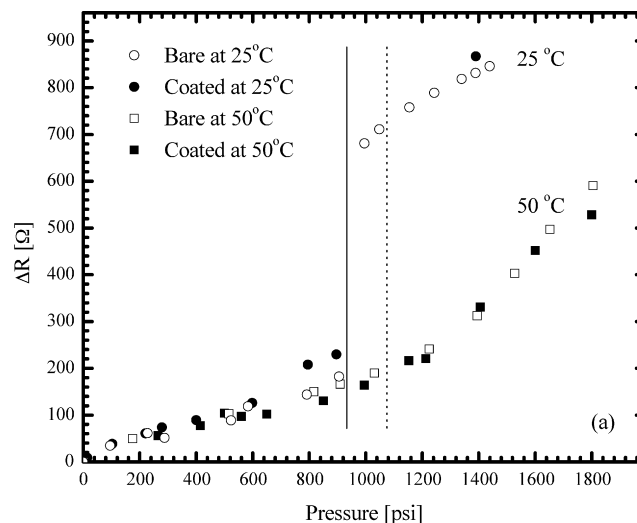


Fig. 4. Resistance change for bare and PFOMA-coated QCM crystals as a function of (a) pressure and (b) CO₂ density–viscosity product.

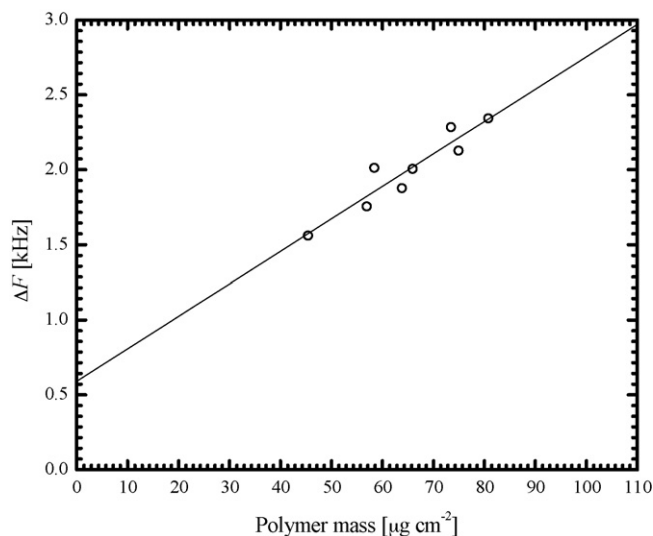


Fig. 5. Frequency change due to absorption of CO₂ in polymer film at 1110 psi and 37 °C as a function of initial polymer amount.

(1) can be rewritten for the interval of CO₂ swelling as:

$$\Delta F = F^{\text{vac}} - F^{P_m} = S\Delta F_f + \Delta F_{\text{ads}} + \Delta F_P + \Delta F_\eta \quad (6)$$

Here, CO₂ sorption has been split into two contributions: adsorption on the surface (ΔF_{ads}), and absorption into the polymer ($S\Delta F_f$). Therefore, the slope of the linear plot of ($F^{\text{vac}} - F^{P_m}$) versus ΔF_f indicates the solubility (absorption) of CO₂ in the polymer film (S). The intercept of the plot reflects other contributions; including the surface adsorption of CO₂ which is expected to be independent of the polymer mass. Such a plot is shown in Fig. 5 from which the solubility (S) of CO₂ in the polymer at 1110 psi and 37 °C is determined to be approximately 0.4 g g⁻¹. Alternatively, the solubility of CO₂ in the polymer was evaluated from the frequency change at different pressures below the experimental dissolution pressure (P_{dis}), where the absorbed mass was obtained from Eqs. (1)–(4), the results are shown in Fig. 6. From this figure, the solubility of CO₂ expected in the polymer at 37 °C and 1100 psi is about 0.48 g g⁻¹. The difference between these two values (0.48 versus 0.4 g g⁻¹) can be attributed to the surface adsorption of CO₂ on the polymer which was not accounted for in the later cases.

Finally, the sorption kinetics of CO₂ can be determined since real time data can be easily obtained with the QCM. The frequency data in the initial stage, prior to dissolution, was fitted to a simple Fickian diffusion model to obtain the diffusivity of CO₂ in PFOMA [42]. As can be seen in Fig. 7, a good fit was obtained with this model. In this graph, the thickness of the polymer was calculated from the ΔF_m and the bulk polymer density (~ 1.1 g/cm³) [43], the diffusion coefficient was fitted and found to be on the order of 1×10^{-9} cm²/s. This value is within the reasonable range of diffusivities for other polymers [44].

4.3. Dissolution-dominated stage

Once the CO₂ concentration in the polymer reaches a critical value, polymer chains start to disentangle from each other and

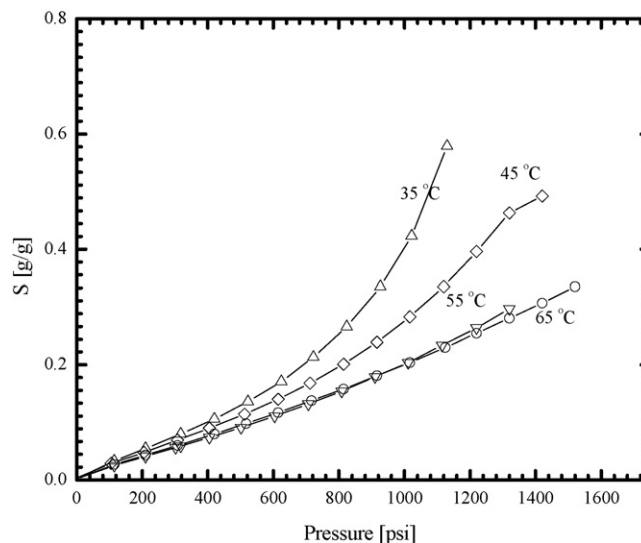


Fig. 6. Solubility (S) of CO₂ in PFOMA at different temperatures as a function of pressure.

dissolution begins. As can be seen from Fig. 6, this critical CO₂ concentration value ranged between 0.3 and 0.6 mass fraction. For a 15 kDa molecular weight PFOMA sample this is translated into 100–200 CO₂ molecules per polymer molecule, or 4–8 CO₂ molecules per repeat unit.

After the steady state frequency at P_m is reached, the CO₂ pressure inside the cell is increased to P_{exp} within a short period of time (about 20–30 s). As the pressure increased to P_{exp} , a combination of adsorption/absorption of the pressurized CO₂ causes the overall frequency to decrease reaching a local minimum, F_{min} , as can be seen in Fig. 2. When the frequency reaches the vicinity of the minimum, the increasingly adsorbed/absorbed amount of CO₂ reaches its critical dissolution density and polymer dissolution starts. The time taken to reach F_{min} depends on the values of P_m and P_{exp} and usually occurs a few seconds before P_{exp} is reached. This minimum may represent the point

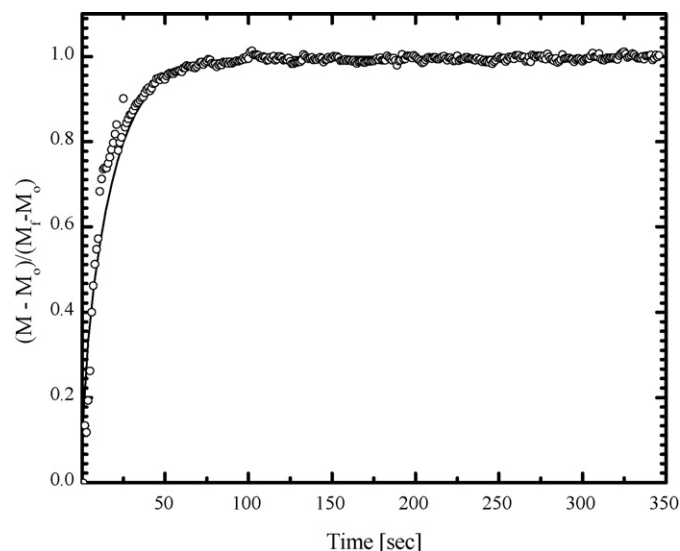


Fig. 7. Sorption kinetics of CO₂ in PFOMA film at 750 psi and 45 °C (circles) with its fit to Fickian diffusion model.

where the absorption/adsorption rate of CO₂ onto/into the film is in equilibrium with the rate of film dissolution. After passing the frequency minimum, the dissolution rate of the polymer is much larger than the CO₂ adsorption/absorption rate; the process becomes dominated by film dissolution. In summary, the whole polymer dissolution process consists of two mechanisms: a short absorption/adsorption-dominated stage as the pressure changes from P_m to P_{exp} , followed by a dissolution-dominated stage under the constant pressure of P_{exp} .

The dissolution stage starts at F_{min} and is continuously monitored until the frequency reaches a new steady state level, $F^{P_{exp}}$, which usually takes 10–60 min depending on the conditions. As the polymer starts to dissolve, the absorbed CO₂ will be released. It should be noted that during the polymer dissolution the pressure and temperature are constant and the frequency change is due only to mass change on the crystal. Therefore, this frequency change can be written as:

$$\Delta F = F_{min} - F^{P_{exp}} = \Delta F_f + \Delta F_{CO_2} = (1 + S)\Delta F_f \quad (7)$$

where ΔF_{CO_2} is the change in frequency due to the net CO₂ mass change in the remaining polymer film. If the small polymer mass loss in the adsorption/absorption-dominated stage is neglected, the total mass change on the crystal in the dissolution stage, calculated from Eq. (7) as m_{dis} , should be larger than m_f , the actual polymer mass removed. This is because m_{dis} accounts for both the dissolved polymer and the change in CO₂ mass, whereas m_f is due to polymer mass only. However, this is not the case, as can be seen in Fig. 8. Experimental observations show that m_{dis} is comparable to m_f and that the difference between m_{dis} and m_f depends on the pressure.

At lower pressures, m_{dis} and m_f are comparable. At these pressures (below P_m) the amount of polymer dissolved is small, thus the amount of CO₂ released with the dissolved polymer will be also small. In addition, increasing the pressure from P_m to P_{exp} increases the CO₂ solubility in the polymer. These two

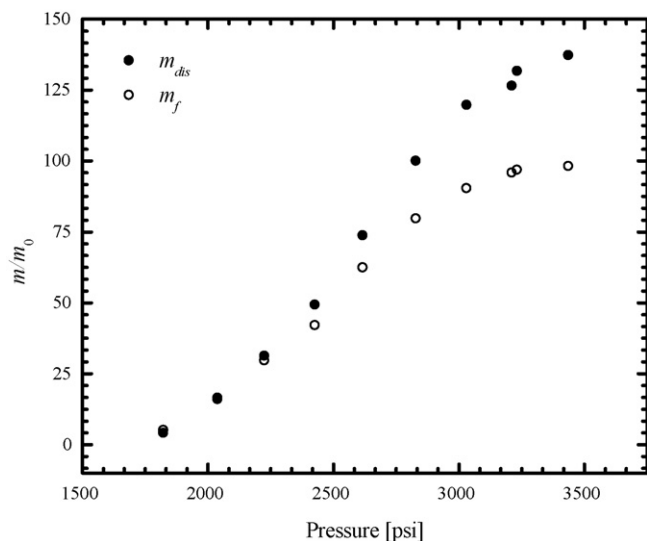


Fig. 8. Comparison between the mass removed during the dissolution process (m_{dis}) and the net polymer mass removed (m_f) for PFOMA at 60 °C as a function of pressure.

factors make the net CO₂ mass contribution negligible. However, at higher pressures there can be a significant difference in the mass associated with the film and the CO₂ on the surface (Fig. 8). This can be explained due to the dramatic increases in the dependency of the polymer dissolution rate on pressure at high pressures. As a result, the remaining film mass on the crystal becomes a small proportion of the total mass coated when the crystal frequency reaches $F^{P_{exp}}$, so that ΔF_{CO_2} is not comparable with $S\Delta F_f$. Therefore, when we determine the net dissolution rate of polymer film, the remaining film mass that can absorb CO₂ should be evaluated in order to eliminate the CO₂ mass contribution to the frequency.

4.4. Polymer dissolution evaluation

In order to compare the different dissolution isotherms, the real-time dissolution results from the QCM were fitted to a simple dissolution model. The simplification comes from the fact that before dissolution starts, the polymer would have been swelled and plasticized with CO₂ for sufficient time to reach equilibrium. Therefore, modeling the dissolution can be simplified by neglecting the diffusion of CO₂ into the polymer film which allows the use of the quasi-stationary dissolution assumption. As a result, the rate of change on the polymer mass can be written as [44]:

$$\frac{1}{A} \frac{dM}{dt} = -k(C_e - C) \quad (8)$$

where M is the remaining mass of the polymer, t the time, A the area, k the mass transfer coefficient, C_e the dissolved concentration in the liquid side, and C is the bulk polymer concentration in CO₂. Writing the concentration as $C = V(M_0 - M)$, where M is the initial polymer mass and V is the CO₂ volume, Eq. (8) can be solved to give:

$$\frac{\Delta M(t)}{M_0} = \frac{M_0 - M(t)}{M_0} = \alpha(1 - e^{-kt}) \quad (9)$$

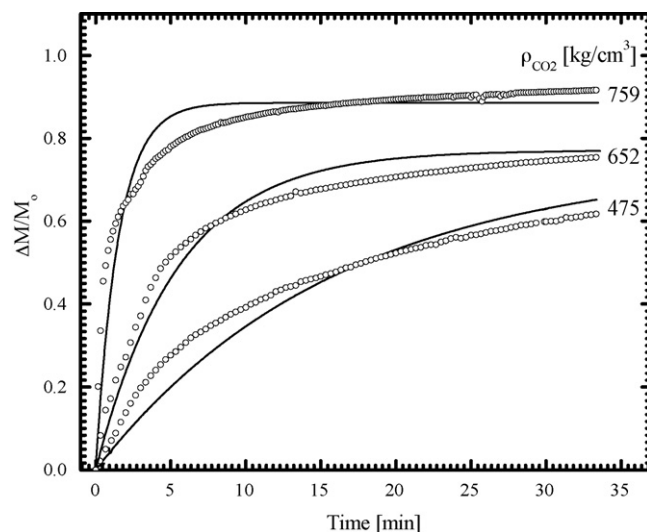


Fig. 9. Time profiles for the mass change for PFOMA films at different CO₂ densities with comparison to their fits to Eq. (9).

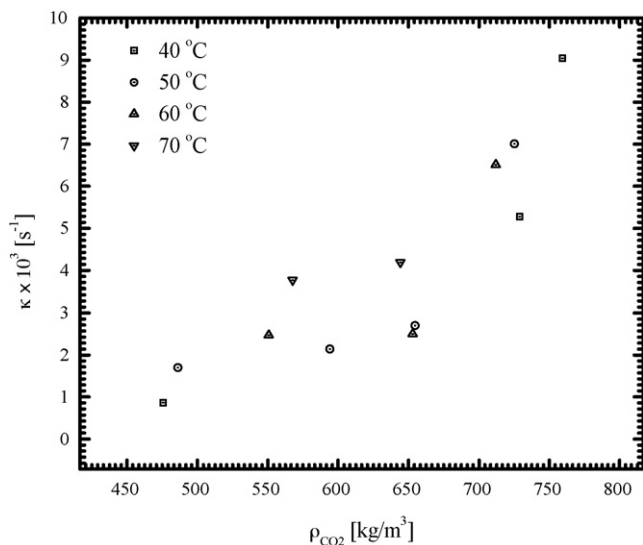


Fig. 10. Dependence of the dissolution rate parameter (κ) on the density of CO_2 at various temperatures.

where $\alpha = VC_0/M_0$ and $\kappa = Ak/V$. The exponential coefficient, κ , can be used to compare the dissolution rates. The value of $\Delta M/M_0$ is calculated from the frequency change as:

$$\frac{\Delta M(t)}{M_0} = \frac{1}{1+S} \frac{\Delta F_m(t)}{\Delta F_f} = \frac{1}{1+S} \frac{F_{P_{\text{exp}}}(t) - F_{\text{min}}}{F_0 - F_{\text{vac}}} \quad (10)$$

The term $1+S$ was used to take into account, in approximate manner, the release of CO_2 as the polymer dissolves into CO_2 as described in Eq. (7). The value of S can be obtained from Fig. 7. Once $\Delta M/M_0$ is known as a function of time, the value of κ can be obtained through non-linear regression. Examples of frequency data manipulated according to Eq. (10) and its fit to Eq. (9) are shown in Fig. 9 from which the parameter κ was estimated.

The dependence of the regressed dissolution rate (κ) on CO_2 density is shown in Fig. 10. While the data is scattered, probably due to the simplified model used, a general trend in the dissolution rate can be seen. As the CO_2 density increases, the value of κ tends to increase. This increase in the dissolution rate with CO_2 density can be attributed to the increase

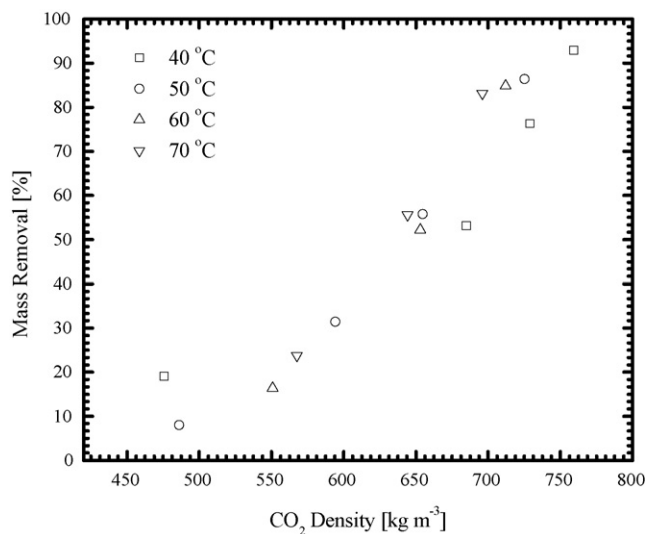


Fig. 11. Amount (%) of total original mass of PFOMA removed after ~ 1 h.

in the solvency power due to the higher concentration of CO_2 molecules around the polymer. It must be noted, however, that temperature seems to play an important role as can be seen, for instance, from the large increase in κ as the temperature changes from 60 to 70 °C. Temperature might affect the dissolution rate by increasing the mobility of the polymer chains. In addition, temperature plays an important role in the interaction energies between all the molecules (polymer–polymer, polymer– CO_2 , and CO_2 – CO_2) [45]. While no kinetic studies on the dissolution of the PFOMA copolymer exist in the literature, a study by Pham et al. [16] on a similar fluorinated copolymer, poly(tetrahydropyranylmethacrylate 1H,1H-perfluorooctyl methacrylate), to the one used in this work confirms the high dependence of dissolution rate on CO_2 density.

Finally, it was observed that complete dissolution of the polymer film was not always achieved as can be seen from Fig. 9. The percentage of the initial mass of PFOMA that was dissolved is plotted in Fig. 11 as a function of CO_2 density. To obtain this figure, the dissolution curve was truncated after 1 h; any polymer remaining on the crystal after such time is considered practically insoluble [16]. At lower densities only a small fraction of

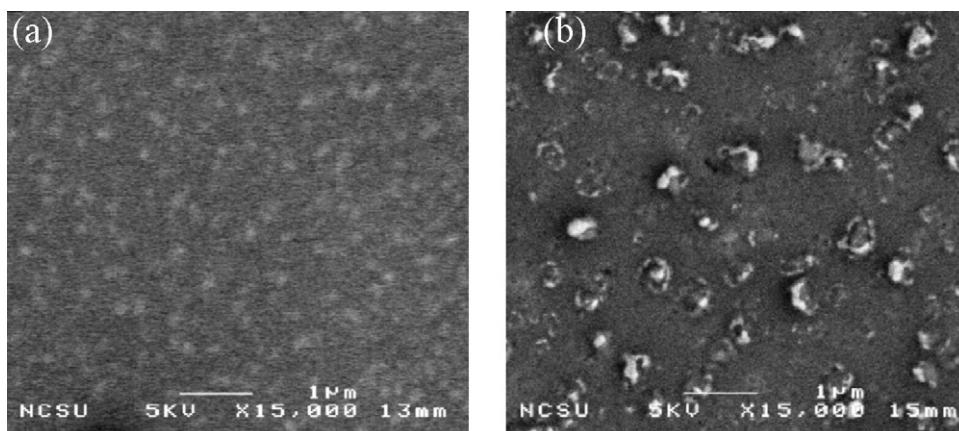


Fig. 12. SEM images for PFOMA-coated QCM crystals before (a) and after (b) dissolution.

the polymer was removed. The maximum removal shown on this figure is 93% which occurs at 759 kg/m³, corresponding to 40 °C and 2000 psi. Again, the effect of density appears to be the most important in determining the amount of polymer removed.

SEM images of the polymer film before and after dissolution (shown in Fig. 12) clearly show the non-soluble parts of the PFOMA. This non-soluble portion of the polymer might be due, for example, to having a high molecular weight or a high degree of entanglement. This suggests that complete removal of the polymer is not practically achievable. On the other hand, the low removal extent at low CO₂ densities is not due solely to thermodynamic effects; it could be a kinetically limited process.

Several studies on copolymers of tetrahydropyranyl methacrylate and fluorinated methylacrylates exist in the literature [42,46] most of which report on the phase behavior and final properties of these copolymers. In addition, studies on the solubility of fluorinated polymers have been reported in order to understand the effect of different functional groups on its solubility in CO₂ [13]. This study provides further insight on the behavior of this class of copolymers, and demonstrates the applicability of QCM in polymer dissolution studies at high pressures.

5. Conclusions

In this study, the dissolution behavior of the fluorinated copolymer poly(FOMA-*r*-THPMA) in supercritical CO₂ was investigated using a quartz crystal microbalance (QCM) over a range of pressures and temperatures. To examine the effect of the polymer film viscoelasticity on the QCM response, the resistance (ΔR) was measured at different temperatures and pressures and comparison was made between coated and uncoated crystals. Based on the linear relation between the QCM resistance change versus the CO₂ density–viscosity product it was concluded that the viscous, non-gravimetric effect was mainly due to viscous coupling with the surrounding fluid, *i.e.*, CO₂, and not the polymer.

An evaluation of the QCM response as CO₂ pressure was increased indicated that the dissolution process consisted of two stages: an absorption-dominated stage followed by a dissolution-dominated stage. Equilibrium and kinetics data provided insight into CO₂–polymer interactions and the resulting dissolution.

From the pressure dependant sorption isotherms the polymer was found to absorb up to 60% of its weight before dissolution commences. Using Fickian diffusion model the diffusivity of CO₂ into the polymer film was estimated to be in the order of 10^{−9} cm²/s; typical range for rubbery polymers.

The PFOMA dissolved in CO₂ at a pressure slightly above the critical pressure at the lowest temperature studied here (40 °C). The dissolution rate and the extent of polymer dissolved depend strongly on temperature and pressure. At low pressures, as little as 20% of the polymer mass was removed during dissolution. This could be attributed to the presence of insoluble polymer regions due to, for example, the molecular weight distribution or high entanglement density. It is also believed that at low pressures the dissolution process becomes kinetically limited and very long times are required to achieve complete dissolution.

We demonstrated here the use of the QCM in the analysis of polymer dissolution in static systems. This analytical tool can also be utilized in analyzing the effect of flowing CO₂ on dissolution in comparison to static system to elucidate the effect of mass transfer on the polymer dissolution. This study is a step towards the understanding and quantification of polymer dissolution in supercritical CO₂ which will help in its successful implementation in different potential applications.

Acknowledgements

We greatly acknowledge the NSF Center for Responsible Solvents and Processes an STC Program of the National Science Foundation under Agreement No. CHE-9876674 and the Kenan Center for Utilization of CO₂ in Manufacturing for financial support. We express our thanks to the DeSimone research group at UNC-Chapel Hill for providing the polymer samples. We also thank the Carbonell research group and Kenan CO₂ Center at NC State University for technical assistance and facility utilization. Finally, we would like to acknowledge Mr. Jonathan Braxton and Mr. John Bedenbaugh undergraduate students of the University of South Carolina. James Kyzar of Mississippi State University, and Ms. Candis A. Collins of NC A&T State University, for their assistance with laboratory experiments. Support for the undergraduate students was provided by NSF Green Processing REU Program (EEC-9912339).

References

- [1] B.A. Miller-Chou, J.L. Koenig, A review of polymer dissolution, *Prog. Polym. Sci.* 28 (2003) 1223–1270.
- [2] D.L. Tomasko, H.B. Li, D.H. Liu, X.M. Han, M.J. Wingert, L.J. Lee, K.W. Koelling, A review of CO₂ applications in the processing of polymers, *Ind. Eng. Chem. Res.* 42 (2003) 6431–6456.
- [3] I. Kikic, F. Vecchione, Supercritical impregnation of polymers, *Curr. Opin. Solid State Mater. Sci.* 7 (2003) 399–405.
- [4] J.M. DeSimone, Practical approaches to green solvents, *Science* 297 (2002) 799–803.
- [5] V.Q. Pham, G.L. Weibel, N.G. Rao, C.K. Ober, Dissolution rate measurements for resist processing in supercritical carbon dioxide, in: *Proceedings of SPIE—The International Society for Optical Engineering*, 2002.
- [6] J.N. Hay, A. Khan, Review—environmentally friendly coatings using carbon dioxide as the carrier medium, *J. Mater. Sci.* 37 (2002) 4841–4850.
- [7] D.K. Taylor, R. Carbonell, J.M. DeSimone, Opportunities for pollution prevention and energy efficiency enabled by the carbon dioxide technology platform, *Annu. Rev. Energy Environ.* 25 (2000) 115–146.
- [8] J.B. McClain, D.E. Betts, D.A. Canelas, E.T. Samulski, J.M. DeSimone, J.D. Londono, H.D. Cochran, G.D. Wignall, D. ChilluraMartino, R. Triolo, Design of nonionic surfactants for supercritical carbon dioxide, *Science* 274 (1996) 2049–2052.
- [9] J.M. Desimone, E.E. Maury, Y.Z. Menciloglu, J.B. McClain, T.J. Romack, J.R. Combes, Dispersion polymerizations in supercritical carbon-dioxide, *Science* 265 (1994) 356–359.
- [10] T. Sarbu, T. Styranec, E.J. Beckman, Non-fluorous polymers with very high solubility in supercritical CO₂ down to low pressures, *Nature* 405 (2000) 165–168.
- [11] D. Patterson, Polymer compatibility with and without a solvent, *Polym. Eng. Sci.* 22 (1982) 64–73.
- [12] F. Rindfleisch, T.P. DiNoia, M.A. McHugh, Solubility of polymers and copolymers in supercritical CO₂, *J. Phys. Chem.* 100 (1996) 15581–15587.
- [13] M.A. McHugh, A. Garach-Domech, I.-H. Park, D. Li, E. Barbu, P. Graham, J. Tsibouklis, Impact of fluorination and side-chain length on

- poly(methylpropenoxyalkylsiloxane) and poly(alkyl methacrylate) solubility in supercritical carbon dioxide, *Macromolecules* 35 (2002) 6479–6482.
- [14] P.T. Raveendran, S.L. Wallen, Exploring CO₂-philicity: effects of stepwise fluorination, *J. Phys. Chem. B* 107 (2003) 1473–1477.
- [15] K.J. Wynne, S. Shenoy, T. Fujiwara, S. Irie, D. Woerdeman, R. Sebra, A. Garach, M. McHugh, Supercritical and liquid CO₂: polymer swelling and effects on melting behavior, *Polym. Preprints* 43 (2002) 888.
- [16] V.Q. Pham, N. Rao, C.K. Ober, Swelling and dissolution rate measurements of polymer thin films in supercritical carbon dioxide, *J. Supercrit. Fluids* 31 (2004) 323–328.
- [17] D.C. Bonner, Y.L. Cheng, New method for determination of equilibrium sorption of gases by polymers at elevated temperatures and pressures, *J. Polym. Sci.: Polym. Lett. Ed.* 13 (1975) 259–264.
- [18] S.M. Sirard, P.F. Green, K.P. Johnston, Spectroscopic ellipsometry investigation of the swelling of poly(dimethylsiloxane) thin films with high pressure carbon dioxide, *J. Phys. Chem. B* 105 (2001) 766–772.
- [19] Y.-T. Wu, C.S. Grant, Microweighing in supercritical carbon dioxide, in: J.A. Schwarz, C.I. Contescu, K. Putyera (Eds.), *Dekker Encyclopedia of Nanoscience and Nanotechnology*, Marcel Dekker, Inc., New York, 2004, pp. 1977–1990.
- [20] J.H. Aubert, Solubility of carbon dioxide in polymers by the quartz crystal microbalance technique, *J. Supercrit. Fluids* 11 (1998) 163–172.
- [21] K. Otake, S. Kurosawa, T. Sako, T. Sugeta, M. Hongo, M. Sato, Frequency change of a quartz crystal microbalance at the supercritical condition of carbon dioxide, *J. Supercrit. Fluids* 7 (1994) 289–292.
- [22] K. Miura, K. Otake, S. Kurosawa, T. Sako, T. Sugeta, T. Nakane, M. Sato, T. Tsuji, T. Hiaki, M. Hongo, Solubility and adsorption of high pressure carbon dioxide to poly(styrene), *Fluid Phase Equilib.* 144 (1998) 181–189.
- [23] S.E. Guigard, G.L. Hayward, R.G. Zytner, W.H. Stiver, Measurement of solubilities in supercritical fluids using a piezoelectric quartz crystal, *Fluid Phase Equilib.* 187 (2001) 233–246.
- [24] C. Zhang, B.P. Cappleman, M. Defibaugh-Chavez, D.H. Weinkauff, Glassy polymer-sorption phenomena measured with a quartz crystal microbalance technique, *J. Polym. Sci. Part B: Polym. Phys.* 41 (2003) 2109–2118.
- [25] M. Naito, Y. Sasaki, T. Dewa, Y. Aoyama, Y. Okahata, Effect of solvation on induce-fit molecular recognition in supercritical fluid to organic crystals immobilized on a quartz crystal microbalance, *J. Am. Chem. Soc.* 123 (2001) 11037–11041.
- [26] R.M. Oag, P.J. King, C.J. Mellor, M.W. George, J. Ke, M. Poliakoff, Probing the vapor–liquid phase behaviors of near-critical and supercritical fluids using a shear mode piezoelectric sensor, *Anal. Chem.* 75 (2003) 479–485.
- [27] J. Ke, P.J. King, M.W. George, M. Poliakoff, Method for locating the vapor–liquid critical point of multicomponent fluid mixtures using a shear mode piezoelectric sensor, *Anal. Chem.* 77 (2005) 85–92.
- [28] V. Carla, K. Wang, Y. Hussain, K. Efimenko, J. Genzer, C. Grant, G.C. Sarti, R.G. Carbonell, F. Doghieri, Nonequilibrium model for sorption and swelling of bulk glassy polymer films with supercritical carbon dioxide, *Macromolecules* 38 (2005) 10299–10313.
- [29] Y.A. Hussain, Supercritical CO₂ Aided Processing of Thin Polymer Films Studied using the Quartz Crystal Microbalance, in *Chemical and Biomolecular Engineering*, North Carolina State University, Raleigh, 2006, p. 234.
- [30] W. Hinsberg, F.A. Houle, S.-W. Lee, H. Ito, K. Kanazawa, Characterization of reactive dissolution and swelling of polymer films using a quartz crystal microbalance and visible and infrared reflectance spectroscopy, *Macromolecules* 38 (2005) 1882–1898.
- [31] H. Ito, Dissolution behavior of chemically amplified resist polymers for 248-, 193-, and 157-nm lithography, *IBM J. Res. Dev.* 45 (2001) 683–695.
- [32] G. Sauerbrey, Use of quartz vibration for weighing thin films on a microbalance, *Zeitschrift Fur Physik* 155 (1959) 206–222.
- [33] C.D. Stockbridge, Effects of gas pressure on quartz crystal microbalances, in: K.H. Behrmdt (Ed.), *Vacuum Microbalance Techniques*, Plenum Press, New York, 1966, p. 147.
- [34] K.K. Kanazawa, J.G. Gordon II, The oscillation frequency of a quartz resonator in contact with a liquid, *Anal. Chim. Acta* 175 (1985) 99–105.
- [35] E.A. Klavetter, S.J. Martin, K.O. Wessendorf, Monitoring jet fuel thermal stability using a quartz-crystal microbalance, *Energy Fuels* 7 (1993) 582–588.
- [36] L. Banda, M. Alcoutlabi, G.B. McKenna, Errors induced in quartz crystal mass uptake measurements by nongravimetric effects: considerations beyond the EerNisse caution, *J. Polym. Sci. Part B: Polym. Phys.* 44 (2006) 801–814.
- [37] D.X. Wang, P. Mousavi, P.J. Hauser, W. Oxenham, C.S. Grant, Quartz crystal microbalance in elevated temperature viscous liquids: temperature effect compensation and lubricant degradation monitoring, *Colloids Surf. A: Physicochem. Eng. Aspects* 268 (2005) 30–39.
- [38] D. Wang, P. Mousavi, P.J. Hauser, W. Oxenham, C.S. Grant, A novel testing system for evaluating the thermal stability of polyol ester lubricants, *Ind. Eng. Chem. Res.* 43 (2004) 6638–6646.
- [39] M. Yang, M. Thompson, Surface-morphology and the response of the thickness-shear mode acoustic-wave sensor in liquids, *Anal. Chim. Acta* 9 (1993) 1990–1994.
- [40] Y.T. Wu, P.J. Akoto-Ampaw, M. Elbaccouch, M.L. Hurrey, S.L. Wallen, C.S. Grant, Quartz crystal microbalance (QCM) in high-pressure carbon dioxide (CO₂): experimental aspects of QCM theory and CO₂ adsorption, *Langmuir* 20 (2004) 3665–3673.
- [41] E.N. Hoggan, K. Wang, D. Flowers, J.M. DeSimone, R.G. Carbonell, “Dry” lithography using liquid and supercritical carbon dioxide based chemistries and processes, *IEEE Trans. Semicond. Manuf.* 17 (2004) 510–516.
- [42] J. Crank, *The Mathematics of Diffusion*, 2nd ed., Oxford University Press, London, England, 1975.
- [43] S. Yang, J.G. Wang, K. Ogino, S. Valiyaveetil, C.K. Ober, Low-surface-energy fluoromethacrylate block copolymers with patternable elements, *Chem. Mater.* 12 (2000) 33–40.
- [44] J. Brandup, E.H. Immergut, E.A. Grulke (Eds.), *Polymer Handbook*, 4th ed., Wiley, New York, 1999.
- [45] Z. Cao, S. Kovenklioglu, D.M. Kalyon, R. Yazici, Experimental investigation and modeling of the dissolution of polymers and filled polymers, *Polym. Eng. Sci.* 38 (1998) 90–100.
- [46] J.Y. Heo, J.T. Kim, Y.-S. Jeong, Y.-S. Gal, K.T. Lim, Solubility behavior of copolymers of tetrahydropyranyl methacrylate and 1H,1H,2H,2H-perfluorooctyl methacrylate in carbon dioxide: effect of deprotection of THP groups, *J. Ind. Eng. Chem.* 10 (2004) 389–394.